Available online at www.sciencedirect.com
SCIENCE DIRECT®
Journal of Computational Physics 201 (2004) 421–438
JOURNAL OF COMPUTATIONAL PHYSICS
www.elsevier.com/locate/jcp

How to simulate anisotropic diffusion processes on curved surfaces

Michael Christensen *

Physics Department, SDU – Odense University, Campusvej 55, DK-5230 Odense M, Denmark

Received 11 September 2003; received in revised form 5 April 2004; accepted 7 June 2004
Available online 15 September 2004

Abstract

A general method for simulating diffusive processes in inhomogeneous, anisotropic media or in spaces with non-trivial geometry, such as on irregular metallic surfaces or cellular membranes, is derived through the diffusion approximation leading from the Master equation to the Fokker–Planck equation. The method is of the Monte Carlo type, and it can be applied to multi-particle systems and even coupled to internal dynamics, for example the quantum mechanical development of spin states. The correctness of the algorithm is proved and optimization issues discussed. As an illustration, recombination processes on a curved surface is treated.
© 2004 Elsevier Inc. All rights reserved.

PACS: 02.70.Lq; 02.40.Hw; 60.10.Cb; 82.20.Wt; 82.65.Yh

Keywords: Diffusion: anisotropic, inhomogeneous, at interfaces; Numerical: Monte Carlo, simulation; Surface: Brownian motion on, Riemannian, manifold

1. Introduction

Diffusion processes occur countless times in theoretical and experimental considerations across many fields of science [1], and applications hereof to real life systems are abundant. Unfortunately, only the simplest of systems can be treated analytically, a fact that has spawned a barrage of specialized numerical routines for simulating particle dynamics within the context of statistical mechanics. The majority of these methods are Monte Carlo-based methods as they readily incorporate the statistical nature of the underlying problem [2]. They are somewhat cumbersome on the computational side (CPU time) but they are far easier to extend than many of their analytical/numerical alternatives with respect to particle number, dimension of space, asymmetries of boundary conditions and various properties of the media.

* Corresponding author. Tel.: +45-6550-3513; fax: +45-6550-8760.
E-mail addresses: inane@fysik.sdu.dk, moga@mail.dk (M. Christensen).

0021-9991/$ - see front matter © 2004 Elsevier Inc. All rights reserved.
doi:10.1016/j.jcp.2004.06.005

One of the more popular Monte Carlo approaches is the Metropolis algorithm [3] which can be used to sample any (equilibrium) distribution under quite loose assumptions. Regarding time development of out-of-equilibrium systems, the random walk model is commonly recognized as a correct representation of the single-particle diffusion process in isotropic and homogeneous media with no external forces whenever the step size is suitably small. Kikuchi et al. [4] proved that the incorporation of the Metropolis algorithm into the random walk yields a correct description of the multi-particle diffusion process even in the presence of an external potential. In other words, the applicability of the Metropolis algorithm was expanded from merely equilibrium descriptions to detailed time-development of diffusive systems. Later, the same authors extended their method to include hydrodynamical effects [5], thereby providing an example of an anisotropic and inhomogeneous diffusion process described in Cartesian coordinates.

In a broader perspective, other types of anisotropy and inhomogeneity are relevant to study, and it is sometimes desirable to use other coordinate systems, for example spherical coordinates. In some cases, such as diffusion on a sphere, a Cartesian system does not even exist. Diffusion processes on manifolds are usually established by rolling a random walk in a flat space onto the surface [6,7]. Theoretically such problems can be solved by considering the flow of diffeomorphisms on the manifold, but the application of these analytical methods is limited to isotropic and homogeneous systems. For most physical systems such considerations are too involved to be carried through anyway. In these setups, it is tempting to apply some ad hoc simulation scheme permuting random coordinates slightly and repeatedly, but unless extreme care is taken, such computational techniques almost certainly represent a diffusion operator different from what was originally intended.

The work in this paper suggests an alternative approach to simulations of diffusive processes in general. Anisotropic effects are modeled differently from Kikuchi et al. [4,5] in a way which in some cases is more efficient and in the isotropic case collapses into the existing description. Like its predecessors, it is capable of performing time-development of multi-particle diffusive systems subjected to (possibly non-conservative) forces in anisotropic and inhomogeneous media, and it is easily derived to incorporate coupled processes (potentially involving internal degrees of freedom) such as reaction, scavenging, particle creation and spin dynamics.

Uniquely for the algorithm provided here is its ability to treat spaces of non-trivial geometry thereby facilitating sound models and calculations of particles undergoing Brownian motion on curved surfaces. Examples of such surfaces are liquid–gas interfaces, metallic surfaces, the surface of large proteins, elongated micelles, cellular membranes and nano-tubes/structures. For such systems (or even flat Euclidean systems in non-Cartesian coordinates), ignoring the curvature terms will certainly lead to incorrect descriptions and eventually to wrong results. Thus, coupled with processes such as reaction, active transport, association and dissociation, the new formalism allows a wide range of fascinating models to be treated in detail and, most of all, correctly.

The remaining parts of this presentation focus on the general algorithm and its correctness, during which some familiarity with differential geometry is assumed on part of the reader; see Appendix A or any textbook on continuum mechanics/general relativity. Common traps and pitfalls as well as optimization issues are also discussed, and finally the new territory, inhomogeneous and anisotropic diffusive processes on curved surfaces, is explored in more detail in order to explain some of the elements needed for an actual computation.

2. The numerical method

The starting point of the simulation problem is the diffusion equation, and because curvilinear coordinates in n-dimensional space are to be allowed, a covariant version is needed. Without loss of generality,

one such variant describing the temporal development of a particles probability distribution P is (see [9] for derivation and explanation)

$$\partial_t P = \nabla_i\big(- D^{ij}F_j P + \nabla_j D^{ij} P\big), \tag{1}$$

where ∇_i is the covariant derivative. Here, the summation rule of Einstein is adopted, meaning that an index appearing both raised and lowered implies a summation over all coordinates. The equation above is just the Fokker–Planck equation with the diffusion tensor D^{ij} identified as half of the second jump moments, and with a response to eventual forces satisfying the Einstein relation. Since the diffusion tensor is invertible (it is real, symmetric and has positive eigenvalues), any system for which the diffusion approximation holds can be described by the above equation by suitable definition of the general force. Even in the presence of internal drifts, currents due to the flow of the media, and drifts due to temperature variations, the governing equation can always be cast into the above form. In the simplest setups, F_j is just a force divided by the typical thermal energy, and if it represents a conservative force at constant temperature it can be written as $k_{\mathrm{B}}TF_j = -\nabla_j V$, where V is the potential energy.

The first pitfall of Monte Carlo diffusion simulations consists of confusing the above equation with the traditional diffusion equation. As the Fokker–Planck equation is just a truncation of the Master equation after the second jump-moment, it is easily interpreted in terms of a Monte Carlo update mechanism and vice versa. But Eq. (1) does *not* coincide with the traditional diffusion equation, which has the diffusion tensor moved outside the innermost derivative. While the validity of the traditional equation for dense and especially anisotropic media has been seriously questioned [9], the present topic is not about microscopic details but merely on simulating such details once they have been decided upon.

Whence, if the traditional diffusion equation is insisted upon then the so-called "spurious" term must be re-introduced in order to transform the problem into the form of Eq. (1), allowing the first and second moments to be read off. This means that the force must include an additional term equal to $(D^{-1})_{jk}\nabla_l D^{lk}$ in order to obtain the traditional diffusion equation, just as it was done in [5]. Failure to do so will break the correspondence between the simulation and the macroscopic dynamic equation. For a detailed discussion of the various drift terms, particularly the spurious one, see [1,8,9].

Every Monte Carlo update scheme moving a particle from $\vec{r}_0$ to $\vec{r}$ in Δt inevitably dictates some transition rate $W(\vec{r}|\vec{r}_0)$. The challenge of constructing a correct numerical method is to make the first and second moments of this transition rate match the ones occurring in the desired diffusion equation. Kikuchi et al. [5] provided such schemes in flat space using Cartesian coordinates. Here, an update routine is constructed that can be applied using curvilinear coordinates in spaces of non-trivial geometry as well. It introduces two spatial and two temporal components, in both cases a dimensionless distribution and its related physical scale. Starting with the spatial ingredients, a dimensionless, radial distribution $f(\xi)$ in n dimensions and a typical jump length $l > 0$ must be specified. Together they represent the radial jump distribution in physical space, and as such $f(\xi)$ must have well-defined first and second moments

$$\overline{\xi^m} \equiv \int_0^\infty f(\xi)\xi^{m+n-1}\,\mathrm{d}\xi. \tag{2}$$

Similarly, a dimensionless distribution $h(\zeta)$ over positive values only and a time scale $\tau > 0$ are to be interpreted collectively as the distribution of waiting times between two successive jumps. As a result, the average $\overline{\zeta}$ must exist. For notational convenience the dimensionless diffusion tensor $\hat{b} \equiv \hat{D}\overline{\zeta}\tau/(\overline{\xi^2}l^2)$ is introduced along with the special square root $\hat{b}^{1/2}$ that conserves the principal axes. That is to say, if $\hat{S}$ is a non-singular transformation such that $\hat{S}\hat{b}\hat{S}^{-1} = \mathrm{diag}(\lambda_i)$ then $\hat{b}^{1/2} = \hat{S}^{-1}\mathrm{diag}(\sqrt{\lambda_i})\hat{S}$. The existence of such an $\hat{S}$ is guaranteed by the properties of the diffusion tensor. In the following the symbol

$$\mathscr{A}_n \equiv \left.\frac{\mathrm{d}\mathscr{V}_n}{\mathrm{d}r}\right|_{r=1} = \frac{n\pi^{n/2}}{\Gamma(1+n/2)} \tag{3}$$

denotes the surface area of a unit sphere in n-dimensional space [10]. Similarly $\mathscr{V}_n$ denotes the volume within the same sphere, whereas $\mathscr{V}_{\vec{z}}$ denotes the volume parametrized by some particular coordinate system $\vec{z}$.

Before the update mechanism itself is presented, consider first a specific transition rate for a single particle, which will map the first two moments onto those of Eq. (1) during the transition from the Master to the Fokker–Planck equation.

Proposition 1. *The microscopic transition rate*

$$W(\vec{r}|\vec{r}_0) = \frac{k}{\mathscr{A}_n\sqrt{\det(\hat{b})}} f\left(\left|\hat{b}^{-1/2}\cdot(\vec{r}-\vec{r}_0)/l\right|\right) \min\left(1, \exp(\vec{F}\cdot(\vec{r}-\vec{r}_0))\right) \tag{4}$$

corresponds (*to the second order in* l) *to the macroscopic equation* (1) *when the rate constant* $k = 2n/(\overline{\zeta}\tau)$ *is used.*

Proof. Let $\hat{c} \equiv \hat{b}^{1/2}$ and assume $n > 1$ (the simple special case $n = 1$ yields the same result). The first and second jump moments will now be calculated in order to show that they coincide with the ones appearing in Eq. (1).

According to the local flatness theorem [11], it is possible to pick a locally flat coordinate system around the point $\vec{r}_0$. Without loss of generality this coordinate system can be chosen so that the forces at $\vec{r}_0$ point along the last coordinate only, or such that the coordinate axes coincide with the principal axes of the diffusion tensor, depending on what is more suitable. A further linear coordinate transformation

$$\vec{y} = \hat{b}^{-1/2}(\vec{r}-\vec{r}_0)/l \tag{5}$$

is applied to the definition of the moments, yielding the following intermediate results:

$$\frac{\overline{\Delta x^i}}{\overline{\Delta t}}(\vec{r}_0) \equiv \int_{\mathscr{V}_{\vec{r}}} W(\vec{r}|\vec{r}_0)(x^i - x_0^i)\,\mathrm{d}\mathscr{V}_{\vec{r}} \tag{6}$$

$$= \frac{kl^2}{\mathscr{A}_n}\int_{\mathscr{V}'_{\vec{y}}} f(|\vec{y}|)(\hat{c}\vec{y})^i(\vec{F}\hat{c}\vec{y})\,\mathrm{d}\mathscr{V}_{\vec{y}} + \mathscr{O}(l^3) \tag{7}$$

and

$$\frac{\overline{\Delta x^i \Delta x^j}}{2\overline{\Delta t}}(\vec{r}_0) \equiv \frac{1}{2}\int_{\mathscr{V}_{\vec{r}}} W(\vec{r}|\vec{r}_0)(x^i - x_0^i)(x^j - x_0^j)\,\mathrm{d}\mathscr{V}_{\vec{r}} \tag{8}$$

$$= \frac{kl^2}{2\mathscr{A}_n}\int_{\mathscr{V}_{\vec{y}}} f(|\vec{y}|)\left(\hat{c}\vec{y}\right)^i\left(\hat{c}\vec{y}\right)^j\mathrm{d}\mathscr{V}_{\vec{y}} + \mathscr{O}(l^3), \tag{9}$$

where the prime on the volume in Eq. (7) denotes integration over the parts of the volume where the jump is directed against the direction of the force.

In the chosen coordinates the distribution is, by construction, uniform over all angles whence facilitating an integration in hyper-spherical coordinates. The transformation to hyper-spherical coordinates is

$$\begin{cases} y^{(1)} = r\sin(\theta_{n-2})\sin(\theta_{n-3})\sin(\theta_{n-4})\cdots\sin(\theta_2)\sin(\theta_1)\sin(\phi), \\ y^{(2)} = r\sin(\theta_{n-2})\sin(\theta_{n-3})\sin(\theta_{n-4})\cdots\sin(\theta_2)\sin(\theta_1)\cos(\phi), \\ y^{(3)} = r\sin(\theta_{n-2})\sin(\theta_{n-3})\sin(\theta_{n-4})\cdots\sin(\theta_2)\cos(\theta_1), \\ \cdots \\ y^{(n-2)} = r\sin(\theta_{n-2})\sin(\theta_{n-3})\cos(\theta_{n-4}), \\ y^{(n-1)} = r\sin(\theta_{n-2})\cos(\theta_{n-3}) \\ y^{(n)} = r\cos(\theta_{n-2}), \end{cases} \tag{10}$$

with Jacobian [10]

$$\prod_{m=1}^{n} \mathrm{d}y^m = r^{n-1}\mathrm{d}r\,\mathrm{d}\phi \prod_{m=1}^{n-2} \sin^m(\theta_m)\,\mathrm{d}\theta_m \tag{11}$$

$$\Downarrow$$

$$\mathscr{A}_n = 2\pi \prod_{m=1}^{n-2} \int_0^{\pi} \sin^m(\theta)\,\mathrm{d}\theta \tag{12}$$

Consider the first moments in a locally flat Cartesian coordinate system aligned such that the last coordinate $y^{(n)}$ points in the opposite direction of the force, implying that θ_{n-2} should only be integrated over $[0, \pi/2]$. The radial part is easily integrated to yield the second moment of the distribution f, and using recursive relations like

$$\int \sin^n(ax)\,\mathrm{d}x = -\frac{\sin^{n-1}(ax)\cos(ax)}{an} + \frac{n-1}{n}\int \sin^{n-2}(ax)\,\mathrm{d}x \tag{13}$$

(obtained through integration by parts) the angular part can be calculated with help from Eq. (12). The drift in the first coordinate then becomes

$$\frac{\overline{\Delta x^{(1)}}}{\overline{\Delta t}}(\vec{r}_0) \approx \frac{kl^2}{\mathscr{A}_n}\overline{\xi^2}(\hat{c})_i^{(1)}(\hat{c})_{(n)}^{i}(\vec{F})^{(n)}\frac{\mathscr{A}_n}{2n} = \frac{k\overline{\zeta}\tau}{2n}(\hat{D}\vec{F})^{(1)} \tag{14}$$

and by symmetry the general relation is

$$\frac{\overline{\Delta x^i}}{\overline{\Delta t}}(\vec{r}_0) = \frac{k\overline{\zeta}\tau}{2n}(\hat{D}\vec{F})^i + \mathscr{O}(l^3), \tag{15}$$

where all physical quantities on the right-hand-side must be evaluated at $\vec{r}_0$. These first moments match the first jump moments in Eq. (1) if $k\overline{\zeta}\tau = 2n$.

A coordinate system in which the tensor $\hat{b}$ is diagonal is most suitable when considering the second moment. Transformations and tricks similar to the above eventually lead to

$$\frac{\overline{\Delta x^{(1)}\Delta x^{(1)}}}{2\overline{\Delta t}}(\vec{r}_0) \approx \frac{kl^2}{2\mathscr{A}_n}\overline{\xi^2}(\hat{b})^{(1)(1)}\frac{\mathscr{A}_n}{n} = \frac{k\overline{\zeta}\tau}{2n}(\hat{D})^{(1)(1)} \tag{16}$$

and

$$\frac{\overline{\Delta x^1\Delta x^{(2)}}}{2\overline{\Delta t}}(\vec{r}_0) \approx 0 \tag{17}$$

and once again the general relation

$$\frac{\overline{\Delta x^i \Delta x^j}}{2\overline{\Delta t}}(\vec{r}_0) = \frac{k\overline{\zeta}\tau}{2n}(\hat{D})^{ij} + \mathcal{O}(l^3) \tag{18}$$

matches the second jump moments in Eq. (1) if $k\overline{\zeta}\tau = 2n$. □

Having established the correctness of the transition rate of Proposition 1, the actual routine is just an implementation of Eq. (4) with a suitable scaling of simulation time, $\Delta t \sim 1/k$. According to Kikuchi et al. [4,5] one key difficulty in Monte Carlo approaches is the mapping of the artificial simulation time onto the proper physical time. Superfluous it may seem to incorporate two separate physical scales l and τ, but they actually help to resolve this temporal interpretation issue, and they come in handy during optimizations of the method. In order to make the artificial and physical time equivalent, clearly the four introduced components must be dependent quantities. Since the length scale l is to be used as an expansion parameter, it must be small compared to all relevant length scales of the system. Whence, fixing of the simulation time to reflect the physical time is most easily achieved by tuning τ according to the relation

$$\overline{\xi^2} l^2 \propto 2\mathrm{Tr}(\hat{D})\overline{\zeta}\tau, \tag{19}$$

which emerges from Eq. (18) of the proof.

Drawing on all these results, a valid update mechanism that will move a single particle from an initial position $(\vec{r}, t)$ to $(\vec{r} + \Delta\vec{r}, t + \Delta t)$ in any n-dimensional media can be implemented as follows:

1. At $(\vec{r}, t)$, calculate $\hat{b}^{1/2}$ and $\vec{F}$.
2. Choose a dimensionless waiting time ζ from the distribution h, and set $\Delta t = \zeta\tau/(2n)$.
3. Choose a test step $\Delta\vec{r}$:
   - 3.1. Choose a unit vector $\vec{w}$ from a uniform distribution over all directions.
   - 3.2. Choose a dimensionless, radial jump length ξ from the distribution f.
   - 3.3. Calculate $\Delta\vec{r}$ by moving an arch length $|\hat{b}^{1/2}\vec{w}|\xi l$ in direction $\hat{b}^{1/2}\vec{w}$ along a geodesic.
   - 3.4. Draw a number q from the uniform distribution over the unit interval, $U(0, 1)$.
   - 3.5. If $q > \exp(\vec{F} \cdot (\Delta\vec{r}))$ then set $\Delta\vec{r} = \vec{0}$.
4. Update $(\vec{r}, t) \to (\vec{r} + \Delta\vec{r}, t + \Delta t)$.

Applying this scheme repeatedly, the full time development of a single trajectory can be found. By keeping track of an ensemble of N trajectories, any quantity of interest can be extracted as an average over all the calculated realizations, and the noise should die out as $1/\sqrt{N}$ as in any basic Monte Carlo sampling.

The steps 3.1–3.3 ensure correct second moments, and the steps 3.4–3.5 constitute a Metropolis validation of the test step ensuring the appropriate equilibration between the origin and the destination [2–4]. It is important to use the square root of the diffusion tensor that conserves the principal axes. Another square root in the form of $\hat{O}\hat{b}^{1/2}$, where $\hat{O}$ is orthogonal, will result in transformed moments $\hat{O}\hat{b}\hat{O}^T$ due to the expansion.

Being an expansion parameter, l must be smaller than any other physical length scale involved in the above calculations, [1] including the ones dictated by the presence of physical time scales in combination with the diffusion tensor. On curved surfaces the radius of curvature is another length scale to remember when deciding on a suitable jump length.

By far the hardest part of the above numerical method is step 3.3. The displacement must always follow a geodesic curve through $\vec{r}$ as these represent the locally straight lines. The main reason for doing so is to

[1] Actually, it is the largest eigenvalue of $\hat{b}^{1/2}$ times l that must be small, but picking the right units for the length and time scale usually implies that the components of the diffusion tensor are of order unity.

ensure uniform sampling over all directions in the tangent space to the point $\vec{r}$. Any deviations from these straight lines represent fictitious forces introduced due to theoretical/computational carelessness, see the example of Section 3. By moving along geodesics, the artificial curvature of the coordinate system is neatly extracted from the particle motion. In flat space the displacement is along a simple line $\Delta\vec{r} = \hat{b}^{1/2}\vec{w}\xi l$ even though care must be taken to ensure this (and the randomness of directions) when working in non-Cartesian coordinates.

Analytic solutions of the geodesic equation are next to impossible to find for any point and any direction on a general manifold. Fortunately, as the jump length is quite small, good approximations are easily obtainable. The behavior of the coordinates on a geodesic curve parametrized by arch length λ can be approximated by a Taylor expansion

$$x^i(\lambda) = x^i|_{\vec{r}} + \left.\frac{\mathrm{d}x^i}{\mathrm{d}\lambda}\right|_{\vec{r}} \lambda + \frac{1}{2}\left.\frac{\mathrm{d}^2x^i}{\mathrm{d}\lambda^2}\right|_{\vec{r}} \lambda^2 + \mathcal{O}(\lambda^3). \tag{20}$$

The original coordinate value $x^i|_{\vec{r}}$ is just coordinate i of the starting point $\vec{r}$ of the jump, and the first derivative is simply the unit tangent vector $\vec{w}$. The second-order term is the important curvature term and it is found from the geodesic equation

$$\frac{\mathrm{d}^2x^i}{\mathrm{d}\lambda^2} = -\Gamma^i_{kl}\frac{\mathrm{d}x^k}{\mathrm{d}\lambda}\frac{\mathrm{d}x^l}{\mathrm{d}\lambda}, \tag{21}$$

where Γ^i_{kl} is the Christoffel symbol describing the curvature of the coordinate system; see Appendix A. Higher order terms to the expansion (20) are obtained by differentiation of the geodesic equation (21).

The curvature term is, as will be illustrated in the upcoming section, necessary for the correctness of the method. Unfortunately, it conjures some computational complications in case the coordinate system has a singularity. Such singularities, in contrast to physical singularities of the space itself, always has a sound physical interpretation and with a little care they pose no real threat.

Optimizations are possible. Since any couple of distributions f and h will do under the requirement that the length scale l is suitably small, the simplest and fastest choice is to use fixed steps (delta-functions). Moreover, as the method relies only on the local jump length being much shorter than the smallest local length scale, the jump scale l can be allowed to vary from point to point implying similar variations in τ according to Eq. (19). In other words, as long as the simulation performs many jumps within a region of approximately constant physical characteristics, the central-limit theorem guarantees diffusive behavior. Thus the simulation can be speeded up considerably in inert regions of configuration space (typically far from boundaries and reaction surfaces).

Boundary conditions (reflecting, absorbing or mixed) are trivially implemented for the single particle method above. Internal dynamics can also be introduced, as long as the development of the internal state can be calculated analytically/numerically during the time Δt the particle stays at $\vec{r}$; see [12] for a radical pair example with magnetic polarization. Multi-particle simulations become available too by applying the single particle update scheme to each individual particle using the smallest (local) jump length available in order to fix the synchronization problem. Complications from localization of the inter-particle boundary is discussed in reference [13]. Reaction between particles or at the boundaries can be achieved by introduction of an integral first-order reaction strength κ to be applied at the contact surfaces. The particles may react with probability $1 - \exp(-\kappa\Delta t)$ or an internal survival variable might be decreased a factor $\exp(-\kappa\Delta t)$ in order to achieve better statistics on long time trajectories. In the diffusion controlled extreme the particles always react, and in the opposite situation of no reactivity reflecting boundary conditions are arrived at after geometric considerations.

3. An example: simulation in spherical coordinates

Consider the simple problem of a single particle diffusing in a homogeneous and isotropic 3-dimensional media ($n = 3$). Scaling the time or space suitably, $D^i_j = \delta^i_j$ can be assumed, where δ is the Kronecker delta. The radial distribution is well-known as a function of time

$$P(r)r^{n-1} = \frac{4\pi r^{n-1}}{\sqrt{4\pi Dt}^n} \exp\left(-\frac{r^2}{4Dt}\right) \tag{22}$$

and it is straight-forward to obtain it using a random walk simulation in Cartesian coordinates (x, y, z).

The same simulation in spherical coordinates (r, θ, ϕ) is not as obvious as it might seem at first sight. While the spherical basis vectors at any point can be normalized to form an orthonormal basis $\{\vec{e}_r, \vec{e}_\theta/r, \vec{e}_\phi/(r\sin\theta)\}$, care must still be taken to ensure that the direction is drawn from a uniform distribution. A common misconception is to believe that a spherical transformation of two uniformly picked angles, $(\alpha, \beta) \to (\sin\alpha\cos\beta, \sin\alpha\sin\beta, \cos\alpha)$, results in a uniform distribution over all directions. Isotropic unit vectors can be generated by drawing the coordinates from the univariate, zero-mean normal distribution $N(0, 1)$ followed by normalization [14]. They can also be generated according to the area element Eq. (11), which in 3 dimensions reduce to $(\theta, \phi) = (\arccos(X), \pi Y)$ where $X, Y \in U(-1, 1)$. Alternatively, a Monte Carlo hit'n'miss method can be applied by assigning coordinates from $U(-1, 1)$ and accepting the vector only if the length is less than one before normalization.

The necessity of the curvature term now becomes apparent. If the expansion (20) is truncated after the first order then the method consists simply of perturbing the coordinate set. Consider a jump along the θ coordinate alone. Without the curvature term, the particle will jump from (r, θ, ϕ) to $(r, \theta + \Delta\theta, \phi)$ when trying to move in the direction of $\vec{e}_\theta$. But this means that the particle has moved along a surface of constant radius and not along a straight line in space. A fictitious force directed towards the origin has been introduced. Likewise, a jump along the ϕ coordinate will seem to be influenced by a force that attracts the particle to the z-axis. The possible destination points have not been sampled uniformly. Effectively, the angular and radial motion is decoupled and the angles can therefore be integrated leaving a simple random walk along the radial coordinate with mobility only a third of the mobility of the original problem. Fig. 1 illustrates how well such a first-order simulation compares to the 1-dimensional solution (22).

For exactly the same reasons as emphasized above, simulating diffusion on a sphere by perturbing one of the spherical angles (θ, ϕ) by a small amount repeatedly will not be correct, since displacements in the latter coordinate will follow circles of constant θ instead of great circles (the geodesics of the sphere). Whence an odd force drawing the particle towards the closest pole has erroneously been introduced. Again, the curvature term must be included.

Alternative tricks, such as applying spherical geometry in order to follow great circles [15], or following the tangent plane itself [12] (thereby leaving the sphere) in combination with projection will both, if done carefully, correctly implement the curvature term. Unfortunately, it is not possible to extend these procedures to any surface of less symmetry than the sphere. The new algorithm, however, can be applied for any surface, and it operates with the two coordinates of the sub-manifold only thereby eliminating the need for projections.

Returning to the 3-dimensional random walk, inclusion of the curvature term in Eq. (20) will lead to the following approximate update when using jump length $\lambda = \xi l$:

$$\begin{pmatrix} \Delta r \\ \Delta\theta \\ \Delta\phi \end{pmatrix} = \begin{pmatrix} w^r \\ w^\theta \\ w^\phi \end{pmatrix} \lambda + \frac{1}{2} \begin{pmatrix} r(w^\theta)^2 + r\sin^2\theta(w^\phi)^2 \\ -2w^r w^\theta/r + \sin\theta\cos\theta(w^\phi)^2 \\ -2w^r w^\phi/r - 2w^\theta w^\phi/\tan\theta \end{pmatrix} \lambda^2, \tag{23}$$

where the random directional vector $\vec{w}$ is normalized in the sense

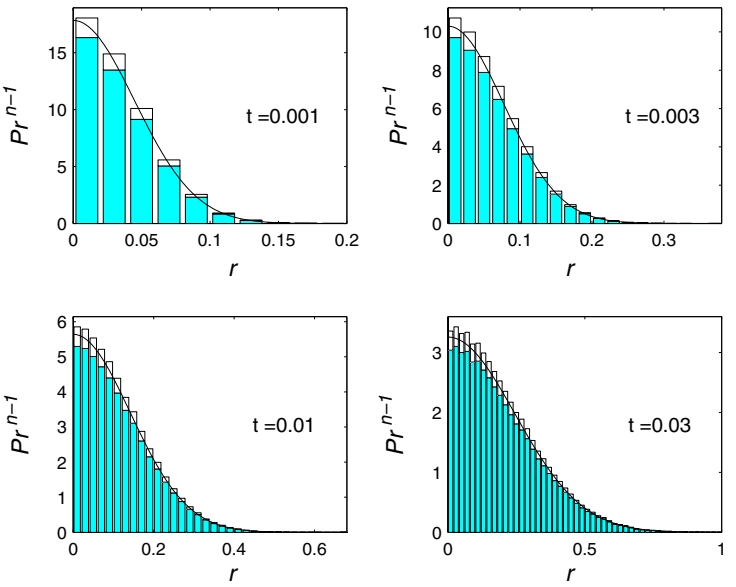

Fig. 1. Radial distribution from a simulation of the 3-dimensional random walk by perturbing random coordinates by a small amount in spherical coordinates while keeping the jump length fixed. Erroneously, it matches the theoretical 1-dimensional distribution instead of the correct 3-dimensional one which can be seen in Fig. 2. The brighter error bars capping the simulation results have a height of 5 standard deviations.

$$|\vec{w}|^2 = (w^r)^2 + r^2(w^\theta)^2 + r^2\sin^2\theta(w^\phi)^2 = 1. \tag{24}$$

Computationally speaking, the addition of the curvature term is not a lot of extra work but the effect is remarkable as illustrated by Fig. 2. The accuracy, as indicated by the error bars, should be good enough for most calculations, but for consistency the small deviation from the analytical result will now be discussed along with possible fixes.

First of all, the update (23) is only an approximation. Third and higher order terms could be added as described in Section 2 at extra computational expense.

Worse, there is a singularity at all points where $r^2\sin\theta = 0$, where the update fails as the second-order term diverges. [2] This singularity is, of course, a singularity of the coordinate system and not a physical singularity; the origin, for example, is just as ordinary as any other point in the flat space. The interpretation is that near $r^2\sin\theta = 0$ it does not make sense to move in all coordinate directions. Close to the origin (small r) any finite jump along an angular basis vector will end up being mainly a radial jump. And near the z-axis (small $r\sin\theta$ with intermediate or large r), any jump along $\vec{e}_\phi$ will mainly be a radial jump or a jump along $\vec{e}_\theta$. In conclusion, near the singularities some coordinates may be ignored (or picked at random) while the others follow the usual update. In terms of Eq. (23), near $r\sin\theta = 0$ a uniform jump subjected to $w^\phi = 0$ is used, and near the origin $w^\theta = 0$ too. Such forceful modifications can be postponed by using smaller and smaller jump lengths when approaching the singularities, thereby increasing the accuracy of the calculation. However, this approach will drastically slow down the computation, and the truncation will eventually have to be applied anyway as the singularity persists.

[2] So does the first-order term due to the factors r and $r\sin\theta$ needed to normalize the angular basis vectors.

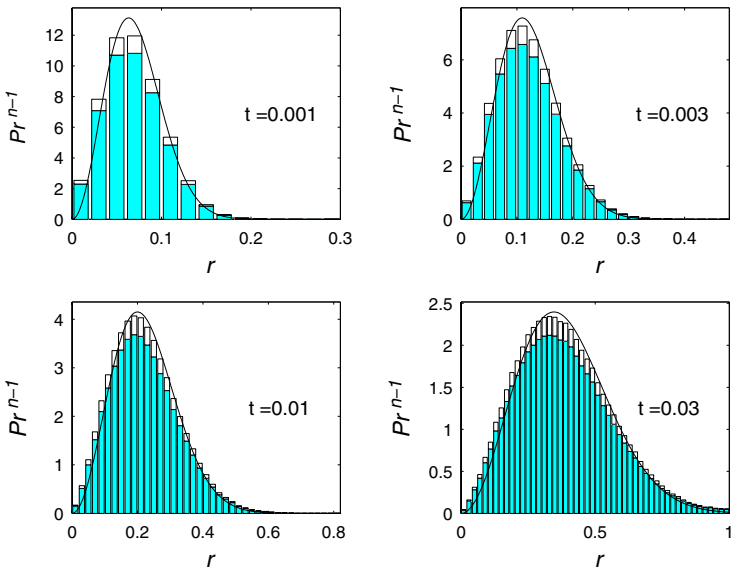

Fig. 2. Radial distribution from a simulation of the 3-dimensional random walk in spherical coordinates by the proposed algorithm including curvature terms. The theoretical 3-dimensional distribution is shown for comparison.

Finally, the actual arch length of the jump given by the update (23) is not exactly λ, though a very good approximation provided l is small. This shifts the time scale slightly during some of the updates according to the relation (19). By requiring the actual displacement to have the desired jump length

$$|\Delta\vec{r}|^2 = \overline{\xi^2} l^2 = \lambda^2 \left(1 + \vec{w} \cdot \frac{\mathrm{d}^2\vec{x}}{\mathrm{d}\lambda^2}\bigg|_{\vec{r}} \lambda + \frac{1}{4} \left(\frac{\mathrm{d}^2\vec{x}}{\mathrm{d}\lambda^2}\bigg|_{\vec{r}} \right)^2 \lambda^2 \right) \tag{25}$$

the correct parameter λ can be found which fixes this problem. A contraction, which leads to acceptable results after only 1–3 iterations, can be crafted from this relation.

Typically, the fixes described here increases the computational time by less than a factor 2 when starting from the simplest (and incorrect) first-order update, thus the present algorithm is feasible compared to simpler and more error-prone methods.

The Metropolis part of the method is absent in this simple example because the potential is constant, but since the present implementation is similar to existing methods, its validity is confirmed in the literature [4]. Application to anisotropic systems can be found in reference [9].

4. An application: diffusion on a curved surface

Until now, the background of the diffusion process has been flat despite the use of various coordinate systems. In order to illustrate how the new-found method works on spaces of non-trivial geometry, a wide family of 2-dimensional surfaces embedded in ordinary 3-dimensional space will now be considered. Generally, two coordinates (u, v) are needed to parametrize the surface. Here, the simplifying assumption is adopted that any radial line (from the origin outward in one direction only) intersects the surface of interest only once. In this way, the spherical angles of the intersection point can be read off, and thus $(u = \theta, v = \phi)$

can be reused as coordinates on the surface. A more direct advantage is that only one map is needed (ignoring minor mathematical technicalities) to get from (u, v)-parameter space to the surface. A surface with only one radial intersection can be parameterized in spherical coordinates as

$$\vec{r} : (\theta, \phi) \to (\gamma(\theta, \phi), \theta, \phi) \tag{26}$$

meaning that the radial coordinate is determined by the two angular ones, $r = \gamma(\theta, \phi)$, where γ is a differentiable function. The two tangents of the surface are orthogonal, and the induced metric tensor, describing the intrinsic geometric properties of the surface (such as defining length and inner product), becomes

$$g_{ij} = \begin{pmatrix} \gamma'^2 + \gamma^2 & \gamma'\dot{\gamma} \\ \gamma'\dot{\gamma} & \dot{\gamma}^2 + \gamma^2 \sin^2\theta \end{pmatrix} \iff g^{ij} = \frac{1}{g}\begin{pmatrix} \dot{\gamma}^2 + \gamma^2 \sin^2\theta & -\gamma'\dot{\gamma} \\ -\gamma'\dot{\gamma} & \gamma'^2 + \gamma^2 \end{pmatrix} \tag{27}$$

with the determinant (square of the volume element)

$$g \equiv \det(g_{ij}) = \gamma^2\left(\dot{\gamma}^2 + (\gamma'^2 + \gamma^2)\sin^2\theta\right). \tag{28}$$

Here the prime and dot denotes differentiation with respect to θ and ϕ, respectively. The resulting Christoffel symbols are

$$\Gamma^{\theta}_{\theta\theta} = \frac{\gamma\gamma'}{g}\left((\gamma'' + \gamma)\gamma \sin^2\theta + 2\dot{\gamma}^2\right), \tag{29}$$

$$\Gamma^{\theta}_{\theta\phi} = \frac{\gamma}{g}\left((\gamma\gamma'\dot{\gamma}' + \gamma^2\dot{\gamma} - \gamma'^2\dot{\gamma})\sin^2\theta + \dot{\gamma}^3 - \gamma\gamma'\dot{\gamma}\cos\theta\sin\theta\right) = \Gamma^{\theta}_{\phi\theta}, \tag{30}$$

$$\Gamma^{\theta}_{\phi\phi} = \frac{\gamma\sin^2\theta}{g}\left(\gamma\gamma'\ddot{\gamma} - \gamma^2\gamma'\sin^2\theta - \gamma^3\sin\theta\cos\theta - 2\gamma'\dot{\gamma}^2 - \gamma\dot{\gamma}^2/\tan\theta\right), \tag{31}$$

$$\Gamma^{\phi}_{\theta\theta} = \frac{\gamma\dot{\gamma}}{g}\left(\gamma\gamma'' - \gamma^2 - 2\gamma'^2\right), \tag{32}$$

$$\Gamma^{\phi}_{\theta\phi} = \frac{\gamma}{g}\left((\gamma'^2 + \gamma^2)\sin\theta(\gamma'\sin\theta + \gamma\cos\theta) + \dot{\gamma}(\gamma\dot{\gamma}' - \gamma'\dot{\gamma})\right) = \Gamma^{\phi}_{\phi\theta}, \tag{33}$$

$$\Gamma^{\phi}_{\phi\phi} = \frac{\gamma\dot{\gamma}}{g}\left(\gamma\ddot{\gamma} + 2\gamma'^2\sin^2\theta + \gamma^2\sin^2\theta + \gamma\gamma'\sin\theta\cos\theta\right). \tag{34}$$

While these symbols might seem cumbersome, bear in mind that the full diffusion operator for such a system is magnitudes more involved. Expanding the covariant derivatives in the diffusion equation (1) will result in an operator containing sums of Christoffel symbols with themselves as well as derivatives of Christoffel symbols. Analytically, it is a nightmare, and computationally, it is a heavy-weight. Direct discretizations will be quite inaccurate, and little hope is left that a transformation into a more decent operator can be found. In that light, the general Monte Carlo diffusion algorithm appears far more straightforward as it applies only the symbols (29)–(34) in linear combinations when constructing the curvature term

$$\begin{pmatrix}\Delta\theta\\ \Delta\phi\end{pmatrix}(\lambda)=\begin{pmatrix}w^\theta\\ w^\phi\end{pmatrix}\lambda+\frac{1}{2}\begin{pmatrix}\Gamma^\theta_{\theta\theta}(w^\theta)^2+2\Gamma^\theta_{\theta\phi}w^\theta w^\phi+\Gamma^\theta_{\phi\phi}(w^\phi)^2\\ \Gamma^\phi_{\theta\theta}(w^\theta)^2+2\Gamma^\phi_{\theta\phi}w^\theta w^\phi+\Gamma^\phi_{\phi\phi}(w^\phi)^2\end{pmatrix}\lambda^2, \tag{35}$$

whereby it achieves the desired jump moments. [3] The special square root of the diffusion tensor should pose no problem either as it can always be calculated analytically:

$$\hat{D}=\begin{pmatrix}a & b\\ b & c\end{pmatrix}\iff \hat{D}^{1/2}=\frac{1}{\sqrt{a+c+2\sqrt{d}}}\begin{pmatrix}a+\sqrt{d} & b\\ b & c+\sqrt{d}\end{pmatrix}. \tag{36}$$

The properties of the diffusion tensor guarantees that the determinant, $d\equiv ac-b^2$, is non-negative.

It is worth considering simplifications of the above results. If the surface has an additional axial symmetry, meaning $\gamma=\gamma(\theta)$, the expressions becomes much simpler. In this case, the metric tensor becomes

$$g_{ij}=\operatorname{diag}\left(\gamma'^2+\gamma^2,\gamma^2\sin^2\theta\right)\iff g^{ij}=\operatorname{diag}\left(\frac{1}{\gamma'^2+\gamma^2},\frac{1}{\gamma^2\sin^2\theta}\right) \tag{37}$$

leading to the Christoffel symbols

$$\Gamma^\theta_{ij}=\begin{pmatrix}\frac{\gamma''+\gamma}{\gamma'^2+\gamma^2}\gamma' & 0\\ 0 & -\frac{\gamma'\sin\theta+\gamma\cos\theta}{\gamma'^2+\gamma^2}\gamma\sin\theta\end{pmatrix}, \tag{38}$$

$$\Gamma^\phi_{ij}=\begin{pmatrix}0 & \frac{\gamma'}{\gamma}+\frac{1}{\tan\theta}\\ \frac{\gamma'}{\gamma}+\frac{1}{\tan\theta} & 0\end{pmatrix}. \tag{39}$$

As a specific example, consider now the axially symmetric surface

$$\gamma(\theta)=1+2(\pi-\theta)^2\sin^2\theta \tag{40}$$

(using some suitable length unit) illustrated in Fig. 3. This surface has a dangerous physical singularity at $\theta=0$ and a more harmless coordinate singularity near $\theta=\pi$. The physical one poses no real problem for the diffusion of any particle of finite size, as there will be a natural limit to how far down the hole at the "north pole" the particle can go due to steric strain. Here, a minimal value of $\theta=\pi/12$ is chosen where an absorbing boundary condition is applied. In this fashion, the valley could be interpreted as an active or catalytic site on a cell or a protein.

Imagine a particle of some type **A** having a high affinity for the surface and therefore diffusing on it. Such a particle could be created anywhere on the surface. It could be created at the active site itself from substrates **B** and **C** diffusing around in 3-dimensional space, $\mathbf{B}+\mathbf{C}\to\mathbf{A}$. It will then leave the site while diffusing on the surface until eventually it returns to the active site and the original process is inverted, $\mathbf{A}\to\mathbf{B}+\mathbf{C}$. This is an example of a recombination process. Another possibility is to have another site, for example at $\theta=\pi$, where particles are created, again by association of substrates from the surrounding space, perhaps by a simple modification, $\mathbf{A}'\to\mathbf{A}$. The particles may be allowed to escape the surface again at this site, and reaction yields of such a process ($\mathbf{A}'\to\mathbf{A}$, diffusion to the other reactive site, $\mathbf{A}\to\mathbf{B}+\mathbf{C}$) could be studied. If the surface is sufficiently good at capturing substrates from the surrounding space, such a trick should speed up site-particle and particle–particle reactions considerably, since it is easier to find the hot spot or another particle in 2 dimensions than it is in 3. Yet again, particles could be allowed to associate

[3] Note how the curvature term for coordinate i can be expressed as an ordinary product of vectors onto a symmetric matrix, $\vec{w}\hat{\Gamma}^i\vec{w}$.

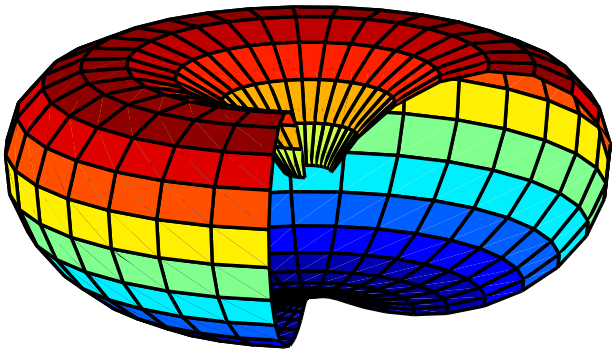

Fig. 3. Example defined by Eq. (40) of a curved surface on which a diffusion process could occur. Valid angles are $\theta \in [\pi/12, \pi]$ and $\phi \in [0, 2\pi]$, although a quarter of the surface is not shown in order to allow a peek inside. The point near $\theta = 0$ has been cut out to avoid the physical singularity (the surface is not differentiable), whereas the point $\theta = \pi$ poses no problem despite the coordinate singularity (the volume element vanishes).

anywhere on the surface according to some distribution or some rate, and likewise allowed to dissociate again continuously, or inter-particle reactions could be allowed.

Evidently, lots of models can be build from this setup, and the Monte Carlo method of Section 2 guarantees correspondence with the governing physical equation of motion, no matter what forces are

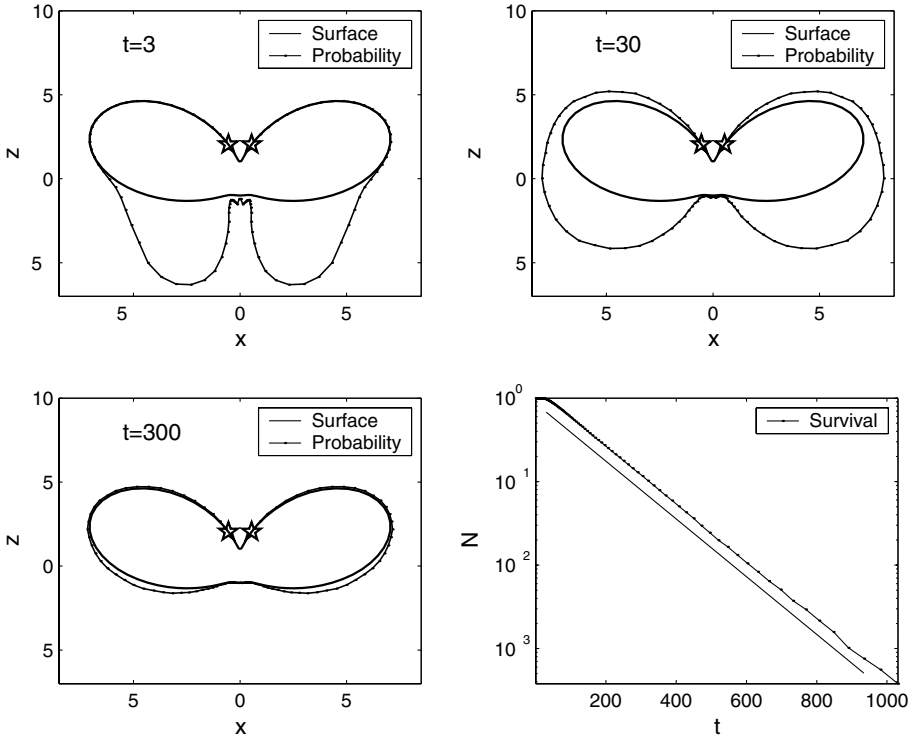

Fig. 4. Time sections and survival probability for a particle initially associated at $\theta = \pi$ then diffusing (in an isotropic and homogeneous fashion) to the opposite pole where it reacts. The stars indicate the diffusion controlled reaction surface $\theta = \pi/12$, the thick line is the surface itself (axial symmetry suppressed), and the probability density at an angle θ is plotted by magnitude perpendicular to the surface at that angle.

applied and regardless of inhomogeneity or anisotropy of the diffusion tensor. The simplest choice is of course to use a potential $V(\theta,\phi)$ implying a conservative force, and an isotropic diffusion tensor $D_i^j = D(\theta,\phi)\delta_i^j$, where $D(\theta,\phi)$ is constant if the media is homogeneous as well.

The diffusion-controlled process of a single particle starting at $\theta = \pi$ and reacting at the $\theta = \pi/12$ boundary on the curved but isotropic and homogeneous surface ($V = 0$) is illustrated in Fig. 4. Relative accuracy of 1% can be achieved within minutes on a personal computer. Similar calculations with non-trivial (and non-axial) potential plus inhomogeneity (all without reaction) show relaxation to the expected equilibrium distribution on the correct timescale.

For the sake of completeness, it should be noted that in simulations with less extreme reactions the analytical contact strength k_0, representing a delta functionality, should be translated into an integral strength κ

$$k_0 = \int k_0 \frac{\delta(r - r_0)}{r^{n-1}} r^{n-1}\,\mathrm{d}r \simeq \kappa \Delta r_{\text{contact}} \tag{41}$$

as the numerical routine expands the reaction surface into a thin reaction volume with a width equal to the average (perpendicular) jump length of the updates leading to collision. For a particle reaching a fixed surface $\Delta r_{\text{contact}} \simeq l/\sqrt{4n}$, and for particle-particle collisions $\Delta r_{\text{contact}} \simeq l/\sqrt{n}$, both with alterations from f and $\hat{D}$.

5. Conclusion

A basic Monte Carlo update mechanism has been presented, which can be used to numerically simulate any single-particle diffusion process in any coordinate system of any space. It is easily extended to cover multi-particle simulations with various types of boundary conditions and even internal dynamics. Tricks, traps and optimization issues of actual simulations have been discussed, and the formulas needed for the treatment of diffusive processes on a large family of surfaces have been provided.

In the literature, a multitude of tailor-made numerical routines has been applied to diffusive systems with high degrees of symmetry. Typically, only Cartesian coordinates, or a single radial coordinate in the case of spherical symmetry, are used. Numerical studies of diffusion on surfaces have mainly been restricted to the plane and the sphere. While such specialized methods may be a little faster (by a constant factor) than the mechanism presented here, they cannot be extended to more general coordinates or to systems of less or no symmetry. Although the principles of diffusion on manifolds has been treated analytically in the literature, almost no guidelines on how to handle inhomogeneity and anisotropy in such cases has been put forth [9].

Compared to the existing algorithms in the literature, the new algorithm has two obvious strengths. First, it allows the simulation to be performed in any coordinate system regardless of the properties of the media, and secondly, this coordinate invariance also allows simulations in non-Euclidean spaces. Even the combination of inhomogeneity and anisotropy of the diffusion tensor on such interfaces is implemented correctly. Whence it opens a huge class of interesting models, especially the study of diffusion processes on curved surfaces in general. For reactions on micellar surfaces, it could be interesting to observe changes in recombination yield induced by squeezing the micelle into an oblong shape. Random walks and reactions on nano-structures can be studied as well.

The proof of the algorithm rests on the transition from the Master equation to the Fokker–Planck equation. It therefore assumes the diffusion approximation to hold [1,16]. This means that the validity of the basic update mechanism cannot be challenged on physical grounds. It is a statistical method like those in references [4,5], and *not* a molecular dynamics simulation [17]. The method does not pass judgement on

the underlying microscopic details or appearance of the diffusion equation. All it relies on is that the first and second jump moments can be calculated and fed to the update routine. Only if the diffusion approximation itself does not hold is the present description insufficient. In that unfortunate case, a unique expansion scheme exists [1,18] from which higher order corrections to the diffusion Eq. (1) can be obtained. Whether an extension to the basic update mechanism exits, which incorporates such higher orders, is a subject for future work.

Acknowledgements

The author thank the two anonymous referees for their very constructive criticism.

Appendix A. A differential geometry tutorial

The notation and formalism of differential geometry is not as well known as its simpler cousin, linear algebra. As a consequence, a short introduction displaying the most basic concepts, relations and techniques is included. The following presentation barely scratches the surface of the extensive mathematics and physics sub-fields, and the reader is advised to explore the literature [6,11,20–22].

A.1. The metric tensor

Imagine an n-dimensional space onto which some spanning coordinate system has been placed. The coordinates are called x^i, where i is an index that runs over the n available coordinate names/numbers. They are just n functions, $x^i(\mathscr{P})$, of the geometrical points, $\mathscr{P}$, in the space [21,22].

Core to the description of any metric space is the concept of the *metric tensor*, also known as the *first fundamental form*. It is the symmetric rank $(0,2)$ tensor, denoted $\hat{g}$, which measures distances in the space. The components of $\hat{g}$ in the chosen coordinate system are called g_{ij} and they do, like every other quantity, depend on the point in which they are measured. The metric defines an operation called *contraction* which is just a generalized inner product. Especially, the product of two vectors – contravariant tensors of rank $(1,0)$ – u^i and v^i is defined as

$$(\vec{u},\vec{v}) \equiv g_{ij}u^i v^j, \tag{A.1}$$

which in turn defines the notion of length through $|\vec{v}|^2 = (\vec{v},\vec{v})$. Here the Einstein notation (from his geometro-dynamic theory) has been used, meaning that every time the same index appears both as a super- and a sub-index, a summation over all coordinates is implied [11,20]. The transformation from vectors to oneforms – covariant tensors of rank $(0,1)$ – is achieved by contraction with the metric tensor, $v_i = g_{ij}v^j$. The reverse transformation, from oneform to vector, requires a similar contraction with the inverse metric tensor of rank $(2,0)$, $\hat{g}^{-1}$, with components g^{ij}, satisfying $g_{ij}g^{jk} = g_i^k = \delta_i^k$, where δ is the Kronecker delta. The above transformations can of course be applied to any tensor of arbitrary covariant/contravariant rank as indices are simply raised and lowered by contraction with the (inverse) metric. Whence only the total rank of a tensor (number of free indices) is usually referred to.

Finally, this special tensor carries all details about the intrinsic geometry of the space, whether it is flat or curved, and if so, exactly how much. The volume element, for example, is just the square root of the determinant of the metric tensor.

A.2. The covariant derivative

Relations between physical quantities must be *covariant*, meaning that they must involve only tensors of similar transformation properties, in order to be valid in any curvilinear coordinate system. The major problem with physical equations when it comes to achieving covariance is that they often contain derivatives, and partial derivatives are not covariant. [4] This is why a *covariant derivative* is introduced, which derives any quantity needed while at the same time keeping track of how much of the change was caused by the weirdness of the coordinate system and how much was an actual change in the quantity of interest. The definition [11] is

$$\nabla_m T^{pq\cdots}_{ij\cdots} \equiv \partial_m T^{pq\cdots}_{ij\cdots} + \Gamma^p_{mr} T^{rq\cdots}_{ij\cdots} + \Gamma^q_{mr} T^{pr\cdots}_{ij\cdots} + \cdots - \Gamma^k_{mi} T^{pq\cdots}_{kj\cdots} - \Gamma^k_{mj} T^{pq\cdots}_{ik\cdots} - \cdots, \tag{A.2}$$

where the *Christoffel symbols*

$$\Gamma^k_{ij} \equiv \tfrac{1}{2} g^{kl}\left(\partial_i g_{lj} + \partial_j g_{il} - \partial_l g_{ij}\right) \tag{A.3}$$

are derivable from the metric tensor. By definition, the Christoffel symbols are symmetric in the two lowered indices but they are not themselves tensors. Furthermore, the covariant derivative on the metric tensor itself is zero.

The most obvious use of the covariant derivative is for defining what is understood by straight lines in curved space. Any curve with tangent u^i is said to be a *geodesic* curve if is satisfies the set of *geodesic equations*:

$$\forall i: \quad u^j \nabla_j u^i = 0. \tag{A.4}$$

It is derived by requiring that the tangent of the curve parallel-transports into itself. Geodesics have extremal arch length and zero extrinsic curvature. They are the locally straight lines of the space.

A.2.1. Spherical coordinates

In 3-dimensional flat Euclidean space the use of Cartesian coordinates (x, y, z) reduces the metric to the identity matrix. Whence the distinction between oneforms and vectors (or any co- or contravariant rank) is minimal — a vector and its corresponding oneform have the same components though one is a column and the other a row vector. The Christoffel symbols are all zero and partial derivatives are the same as covariant derivatives.

Changing coordinates to spherical coordinates (r, θ, ϕ) through the transformation

$$(x = r\sin\theta\cos\phi, y = r\sin\theta\sin\phi, z = r\cos\theta) \tag{A.5}$$

the metric and the inverse become

$$g_{ij} = \operatorname{diag}\left(1, r^2, r^2\sin^2\theta\right) \quad \Longleftrightarrow \quad g^{ij} = \left(1, 1/r^2, 1/(r^2\sin^2\theta)\right) \tag{A.6}$$

with volume element $\sqrt{\det(\hat{g})} = r^2\sin\theta$. The only non-zero Christoffel-symbols are:

[4] Example: In Euclidean space the differential equation for a straight line looks very different in Cartesian coordinates and (hyper)-spherical coordinates when expressed as the constantness of the directional vector.

$$\begin{aligned}
\Gamma^r_{\theta\theta} &= -r,\\
\Gamma^r_{\phi\phi} &= -r\sin^2\theta,\\
\Gamma^\theta_{r\theta} &= 1/r = \Gamma^\theta_{\theta r},\\
\Gamma^\theta_{\phi\phi} &= -\sin\theta\cos\theta,\\
\Gamma^\phi_{r\phi} &= 1/r = \Gamma^\phi_{\phi r},\\
\Gamma^\phi_{\theta\phi} &= 1/\tan\theta = \Gamma^\phi_{\phi\theta},
\end{aligned} \tag{A.7}$$

which are used in the example of Section 3.

A.3. Sub-manifolds

Curved manifolds can be pictured as curved hyper-surfaces embedded in higher dimensional spaces. The embedding of an m-dimensional sub-manifold in an n-dimensional space (obviously with $0 < m < n < \infty$) with metric $g^{(n)}_{ij}$ can be achieved in two ways. Either a set of $n-m$ scalar functions $\{\Phi_A\}_{A=1}^{n-m}$ can be specified, such that the hyper-surface is the set of all solutions to the system of equations $\Phi_A(x^i) = 0$, or alternatively the coordinates can be parametrized by the coordinates ζ^μ on the hyper-surface, $x^i = x^i(\zeta^\mu)$. Here Latin indices are used for the larger space and Greek indices for the embedded space.

A useful basis consists of the m tangents vectors (labeled by μ) of the sub-manifold, $\partial_\mu x^i$, and the $n-m$ normal oneforms (labeled by A), $\partial_i \Phi_A$. From the first fundamental form of the sub-manifold, called the *induced metric*,

$$g^{(m)}_{\mu\nu} = g^{(n)}_{ij}(\partial_\mu x^i)(\partial_\nu x^j) \tag{A.8}$$

every intrinsic property of the hyper-surface can be calculated. For an example, see Section 4.

References

[1] N.G. van Kampen, Stochastic Processes in Physics and Chemistry, second ed., North-Holland Personal Library, New York, 1992.
[2] S.E. Koonin, Computational Physics, Addison-Wesley, New York, 1986.
[3] M.E.J. Newman, G.T. Barkema, Monte Carlo Methods in Statistical Physics, Clarendon Press, Oxford, 2002.
[4] K. Kikuchi, M. Yoshida, T. Maekawa, H. Watanabe, Metropolis Monte Carlo method as a numerical technique to solve the Fokker–Planck equation, Chem. Phys. Lett. 185 (1991) 335.
[5] K. Kikuchi, M. Yoshida, T. Maekawa, H. Watanabe, Metropolis Monte Carlo method for Brownian dynamics simulation generalized to include hydrodynamic interactions, Chem. Phys. Lett. 196 (1992) 57.
[6] N. Ikeda, S. Watanabe, Stochastic Differential Equations and Diffusion Processes, North-Holland/Kodansha, Amsterdam, 1989.
[7] K.D. Elworthy, Stochastic Differential Equations on Manifolds, in: London Mathematical Society Lecture Note Series, Cambridge University Press, London, 1982.
[8] N.G van Kampen, Diffusion in inhomogeneous media, J. Phys. Chem. Solids 49 (1988) 673.
[9] M. Christensen, J.B. Pedersen, Diffusion in inhomogeneous and anisotropic media, J. Chem. Phys. 119 (2003) 5171.
[10] A. Erdélyi (Ed.), Higher Transcendental Functions, vol. II, McGraw-Hill Book Company, New York, 1953.
[11] C.W. Misner, K.S. Thorne, J.A. Wheeler, Gravitation, W.H. Freeman & Company, New York, 1973.
[12] U.E. Steiner, J.Q. Wu, Electronic spin relaxation of photochemically generated radical pairs diffusing in micellar supercages, Chem. Phys. 162 (1992) 53.
[13] P.E. Kloeden, E. Platen, H. Schurz, Numerical Solution of SDE Through Computer Experiments, Springer, Berlin, 1994.
[14] L. Devroye, Non-Uniform Random Variate Generation, Springer, New York, 1986.
[15] J.B. Pedersen, Monte Carlo calculation of ESR line shapes in the slow motional region, J. Chem. Phys. 57 (1972) 2680.
[16] J. Keilson, J.E. Storer, On Brownian motion, Boltzmann's equation, and the Fokker–Planck Equation, in [19], p. 298.
[17] D.L. Ermak, J.A. McCammon, Brownian dynamics with hydrodynamic interactions, J. Chem. Phys. 69 (1978) 1352.
[18] N.G. van Kampen, A Power Series Expansion of the Master Equation, in [19], p. 315.

[19] I. Oppenheimer, K.E. Shuler, G.H. Weiss (Eds.), Stochastic Processes in Chemical Physics: The Master Equation, The MIT Press, Massachusetts, 1977.
[20] G.F.R. Ellis, S.W. Hawking, The Large Scale Structure of Space-time, Cambridge University Press, London, 1997.
[21] L.P. Eisenhart, Riemannian Geometry, Princeton University Press, New York, 1950.
[22] T.J. Willmore, Total Curvature in Riemannian Geometry, John Wiley & Sons, New York, 1982.